Journal Pre-proofs


# The effects of addition of functional monomers and molecular imprinting on dual drug release from intraocular lens material

Ana Topete, Isabel Barahona, Luís F. Santos, Carlos A. Pinto, Jorge A. Saraiva, Ana Paula Serro, Benilde Saramago

PII: S0378-5173(21)00318-5
DOI: https://doi.org/10.1016/j.ijpharm.2021.120513
Reference: IJP 120513

To appear in: *International Journal of Pharmaceutics*

Received Date: 13 January 2021
Revised Date: 13 March 2021
Accepted Date: 17 March 2021

Please cite this article as: A. Topete, I. Barahona, L.F. Santos, C.A. Pinto, J.A. Saraiva, A. Paula Serro, B. Saramago, The effects of addition of functional monomers and molecular imprinting on dual drug release from intraocular lens material, *International Journal of Pharmaceutics* (2021), doi: https://doi.org/10.1016/j.ijpharm.2021.120513

# The effects of addition of functional monomers and molecular imprinting on dual drug release from intraocular lens material

Ana Topete[a], Isabel Barahona[b], Luís F. Santos[a], Carlos A. Pinto[3], Jorge A. Saraiva[c], Ana Paula Serro[a,b*], Benilde Saramago[a]

[a] Centro de Química Estrutural, Departamento de Engenharia Química, Instituto Superior Técnico, Universidade de Lisboa, Av. Rovisco Pais, 1049-001 Lisboa, Portugal
[b] Centro de Investigação Interdisciplinar Egas Moniz, Instituto Universitário Egas Moniz, Quinta da Granja, Monte de Caparica, 2829-511 Caparica, Portugal
[c] QOPNA & LAQV-REQUIMTE, Department of Chemistry, University of Aveiro, Aveiro, Portugal

*Corresponding author: anapaula.serro@tecnico.ulisboa.pt

## Abstract

Although cataract surgery is considered a safe procedure, post-surgery complications such as endophthalmitis and ocular inflammation, may occur. To prevent this, antibiotics and anti-inflammatories are prescribed in the form of eye drops during the post-operatory period, but they lead to a low drug bioavailability in target tissues. The objective of this work is to develop an intraocular lens (IOL) material to deliver simultaneously one antibiotic, moxifloxacin (MXF), and one anti-inflammatory, diclofenac (DFN), in therapeutic concentrations to prevent both complications. The IOL material was modified through the incorporation of functional monomers, as well as molecular imprinting with both drugs using the same functional monomers, namely acrylic acid (AA), methacrylic acid (MAA), 4-vinylpiridine (4-VP) and a combination of MAA+4-VP. The best results were obtained with MAA. Molecular imprinting did not influence the drug release, except with AA. Application of a mathematical model predicted that the released MXF and DFN concentrations would stay above the pre-determined MIC of *S. aureus* and *S. epidermidis* and the minimum values of IC50 of COX-1 and COX-2, for 9 and 14 days, respectively. Antibacterial tests showed that the released antibiotic remained active. The physical properties of the drug-loaded MAA-hydrogel remained adequate. The developed system proved to be non-irritant and non-cytotoxic.

**Keywords:** intraocular lens, moxifloxacin, diclofenac, drug delivery, functional monomers

## 1. Introduction

Cataract surgery is one of the most common surgical procedures worldwide (Fintelmann and Naseri, 2010; Haripriya et al., 2017). The number of operations carried out, per year, reaches 4000 to 6000 per million people in developed countries (Foster et al., 2000). In spite of being a very frequent procedure, it is not free of risks. Endophthalmitis, although rare (incidence 0.03 % - 0.70 %), is a devastating postsurgical intraocular infection that can lead to visual loss (Fintelmann and Naseri, 2010; Haripriya et al., 2017). Postsurgical ocular inflammation is another recurrent issue that can cause pain, photophobia and increase the risk of elevated intraocular pressure, posterior capsule opacification (PCO), cystoid macular edema (CME) and corneal edema, if not treated adequately (Aptel et al., 2017). To prevent endophthalmitis and ocular inflammation, a combination of an antibiotic and a non-steroidal anti-inflammatory drug (NSAID) is usually prescribed in the form of eye drops: topical antibiotics are administered during 1-2 weeks after surgery, while topical NSAIDs are used during 2-4 weeks (Burling-Phillips, 2013; Haripriya, 2017). However, eye drops face several constrains related with the high tear fluid turnover rate, blinking, nasolacrimal drainage and anatomical barriers that reduce the drug ocular bioavailability to less than 5% of the applied dose (Gaudana et al., 2010; Gote et al., 2019; Patel, 2013). Furthermore, the administration of eye drops can be challenging to elderly people, who make up a large percentage of the patients undergoing this procedure. In their case, due to physical or cognitive limitations, the therapy compliance may decrease, leading to an increased risk of postsurgical complications (Matossian, 2020).

In the past few years, intraocular lenses (IOLs) implanted during cataract surgery have been explored as drug delivery systems to avoid eye drops prophylaxis. However, several concerns raise when dealing with this kind of devices. The amount of drug released must be enough to ensure therapeutic concentrations and the drug release profile has to be controlled and extended to achieve the desired effect. Several strategies have been attempted to incorporate drug into the IOL materials and to ensure a sustained drug release, namely, supercritical impregnation (González-Chomón et al., 2012), surface modifications (Anderson et al., 2009; Manju and Kunnatheeri, 2010), attachment of drug reservoirs to the IOL haptic (Eperon et al., 2008; Garty et al., 2011) or to the IOL periphery (Tan et al., 2016), and incorporation of drug-loaded nanoparticles (Huang et al., 2013). The simplest way to incorporate drug into the lens is by soaking it into the drug loading solution, but several research groups followed this strategy and fell short of the therapeutic needs (Kleinmann et al., 2006; Lipnitzki et al., 2013). Drug incorporation highly depends on the properties of the IOL material and the affinity of the drug to the polymeric matrix. In previous works, our group demonstrated that the time and the temperature of the soaking step are important factors (Topete et al., 2018), and found optimized loading conditions to obtain simultaneous release of the antibiotic, moxifloxacin (MXF), and the NSAIDs, diclofenac (DFN) or ketorolac (KTL), from acrylic based hydrogels for IOLs (Topete et al., 2019). While the combination of MXF+KTL attained therapeutic levels for both drugs, the amount of MXF released from the hydrogels loaded with MXF+DFN dropped below the minimum inhibitory concentrations (MICs) of *Staphylococcus aureus* (*S. aureus*) and *Staphylococcus epidermidis* (*S. epidermidis*), two of the most common bacteria colonizers of the eye, after 3 days. A strategy that can be used to enhance the drug loading and improve the drug release profiles is molecular imprinting. Drug imprinted polymers have specific recognition sites for a template molecule (in this case, the drug molecule), resulting in a stronger interaction with such molecule and consequent increased drug loading capacity (Zaidi, 2016a). The imprinted polymers are prepared by mixing the backbone monomers, the cross-linker, the template molecule (the drug) and functional monomers with affinity for the template. During polymerization, the functional monomers rearrange around the drug molecules, creating recognition sites. After polymerization, the material is washed to completely remove the template molecules, leaving empty cavities with binding sites for

the drug. When the material is soaked in the drug solution, the drug molecules diffuse into the polymeric matrix and accommodate in the imprinted cavities. (Alvarez-Lorenzo et al., 2010; Nichols et al., 2018; Zaidi, 2016b). To our knowledge, molecular imprinting was never attempted to produce drug-loaded IOLs, however it has been widely used to increase the drug loading capacity of soft contact lenses (SCLs) materials (Tashakori-Sabzevar and Mohajeri, 2015; White and Byrne, 2010). Prednisolone acetate, dorzolamide, ketotifen fumarate, timolol, norfloxacin, hyaluronic acid and diclofenac are among the numerous drugs that were successfully delivered by imprinted silicone and acrylate based SCLs hydrogels, functionalized with different monomers (Tashakori-Sabzevar and Mohajeri, 2015; White and Byrne, 2010). Some authors found that the simple approach of adding functional monomers to the hydrogel matrix, without molecular imprinting, can increase its drug loading capacity and extend the drug release. Andrade-Vivero *et al.* added two different functional monomers, 4-vinylpyridine (4-VP) and N-(3-aminopropyl) methacrylamide (APMA), to poly(2-hydroxyethyl methacrylate) (pHEMA) hydrogels used for SCLs and other biomedical materials with the objective of potentiating the drug loading/release of two NSAIDs (ibuprofen and DFN) and were successful (Andrade-Vivero et al., 2007).

The aim of the present work is to evaluate the effects of the addition of the functional monomers, acrylic acid (AA), methacrylic acid (MAA) and 4-VP, associated or not with molecular imprinting, on the release of MXF+DFN from the commercial acrylic material CI26Y, used in the IOL manufacturing. The chemical structures of the chosen functional monomers and drugs are presented in **Figure 1**.

MXF is a broad-spectrum fluoroquinolone with activity against *Streptococci*, *Staphylococci* and relevant gram negative pathogens. It is normally used to treat keratitis and as a prophylaxis antibiotic in cataract and refractive surgeries (Miller, 2008). DFN is one of the most commonly prescribed NSAIDs to treat inflammation and control pain after cataract surgery, being able to inhibit both cyclooxygenase 1 (COX-1) and 2 (COX-2) enzymes that take part in the inflammation process (Altman et al., 2015; Hoffman et al., 2016).

Both MXF and DFN present carboxylic and amino groups that are able to interact with AA, MAA and 4-VP via hydrogen bonds and ionic interactions (Hammam et al., 2018; Mohajeri et al., 2012). MAA and 4-VP were already used as functional monomers in polymers imprinted with MXF for potentiometric sensors (Hammam et al., 2018), and pH-responsive polymers imprinted with DFN for (Mohajeri et al., 2012). In both cases, polymers based on MAA demonstrated higher affinity for the drugs. AA was also used to produce contact lenses imprinted with MXF, increasing its loading and release capacity (D. Silva, H.C. Sousa, M.H. Gil, L.F. Santos, M. Salema Oom, C. Alvarez-Lorenzo, B. Saramago, n.d.).

After preparation of the materials, drug loading was done by soaking in the optimized conditions described in previous works (Topete et al., 2019, 2018). The material that led to the best drug release profiles was sterilized by high hydrostatic pressure (HHP), a sterilization method whose application in IOLs was recently studied by our group and proved to be efficient (Topete et al., 2020). The effect of sterilization on the drug release profiles was investigated, and the *in vivo* efficacy was predicted using a mathematical model described by Pimenta *et al.* (Pimenta et al., 2018). Several physical and chemical properties were analysed: liquid uptake capacity, transmittance, Young's modulus and the molecular structure. Irritability potential tests and cytotoxicity tests were done to demonstrate the safety of the material. Finally, antimicrobial tests against *S. aureus* and *S. epidermidis* were carried out to check the activity of the released antibiotic MXF.

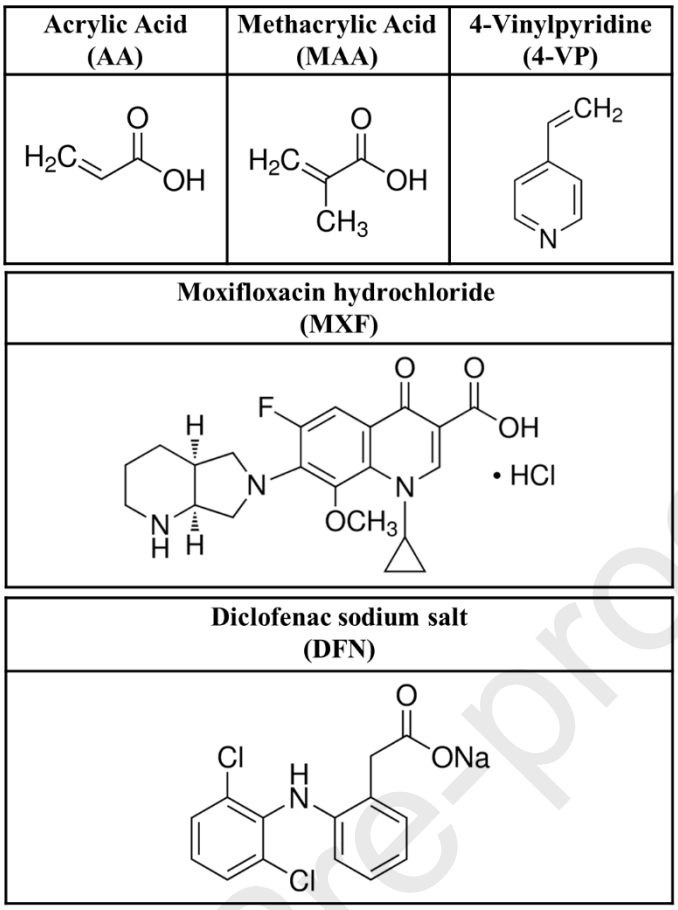


**Figure 1.** Chemical structure of the used functional monomers and drugs.

## 2. Experimental

### 2.1. Materials

The mixture of CI26Y monomers (80-90% of hydroxyethyl methacrylate (HEMA), 10-20% of methyl methacrylate (MMA), <1% of ethanediol dimethacrylate (EGDMA) and <1% of 2-(4-Benzoyl-3-hydroxyphenoxy) ethyl acrylate) was purchased from Contamac (UK). Acrylic acid (AA, purity ≥ 99%) was acquired from Alfa Aesar (USA). Methacrylic acid (MAA, purity ≥ 99%), 4-vinylpyridine (4-VP, purity ≥ 99%) and 2,2′-Azobis(2-methylpropionitrile) (AIBN, purity ≥ 98%) were bought from Sigma Aldrich (USA). Moxifloxacin hydrochloride (MXF, purity ≥ 98%) was obtained from Carbosynth (UK) while diclofenac sodium salt (DFN, purity ≥ 98%) was acquired to Sigma–Aldrich (USA). Phosphate buffer solution (PBS, pH 7.4) was also bought to Sigma-Aldrich (USA). Ethanol (96% v/v) was acquired from Manuel Vieira & C[a] (Portugal). For the antibacterial tests, antimicrobial susceptibility discs and Mueller-Hinton (MH) agar were obtained from Oxoid (UK). For the irritability tests, sodium chloride (NaCl, ≥ 99%) obtained from PanReac AppliChem (Spain) and sodium hydroxide (NaOH, ≥ 99%) purchased from Merck (Germany) were used as controls. For the cytotoxicity tests, the following materials were used: Dulbecco's Modified Eagle's Medium (DMEM), penicillin-streptomycin solution (10000 units/mL of penicillin and 10 mg/mL of streptomycin), calf serum, yellow tetrazolium (3-(4, 5-dimethylthiazolyl-2)-2, 5-diphenyltetrazolium bromide) (MTT), dimethyl sulfoxide (DMSO, ≥ 99%), isopropanol, hydrochloric acid (HCl), NIH/3T3 fibroblasts (93061524) and inserts (6.5 mm) with 8.0

μm pore polycarbonate membrane (Transwell®, Corning), all purchased from Sigma-Aldrich (USA). IGEPAL® was obtained from Merck (Germany). Distilled and deionized (DD) water was obtained using a Millipore system.

### 2.2. Methods

#### 2.2.1. Preparation of the hydrogel samples

To prepare CI26Y hydrogel samples, 4.95 mL of the CI26Y monomers mixture were degassed by ultrasound sonication for 5 minutes and nitrogen bubbling for 15 minutes at room temperature. Then, 52.5 mg of the initiator AIBN was added. The solution was homogenized by magnetic stirring and then poured into a mold of two silanized glasses separated by a spacer with a thickness of 1.0 mm. Polymerization was performed for 18 h at 60 ºC.

To produce the hydrogels with the functional monomers or drug-imprinted (also with functional monomers) the same procedure was followed, but, before the degassing, the monomers alone or with the drugs, were added to the CI26Y mixture and homogenized by magnetic stirring. The compositions of the hydrogels produced are given in **Table 1**. After polymerization, the materials were washed using a soxhlet, with DD water as extraction solvent, for 60 cycles (each cycle corresponding to 20 min). The imprinted materials were additionally washed in ethanol to remove the drugs from the polymeric matrix. Ethanol was eliminated from the samples by evaporation and the samples were rehydrated in water to be cut into disks with a diameter of 5 mm using a punch or in a dumbbell shape appropriate for tensile tests. It shall be stressed that although ethanol leads to an increased swelling of the samples, after its elimination, the samples fully recover their normal swelling behaviour in water. The samples were dried for 3 days at 36 ºC and stored in closed vials until further use.

**Table 1.** Composition of the different hydrogels prepared.

| | | **Blank hydrogel** | **Hydrogels with functional monomers** | | | | **Drug imprinted hydrogels** | | | |
|---|---|---|---|---|---|---|---|---|---|---|
| | | **H** | **HA** | **HM** | **HV** | **HMV** | **HA-I** | **HM-I** | **HV-I** | **HMV-I** |
| **CI26Y mixture (mL)** | | 4.95 | 4.95 | 4.95 | 4.95 | 4.95 | 4.95 | 4.95 | 4.95 | 4.95 |
| **Initiator (AIBN) (mL)** | | 63.94 | 63.94 | 63.94 | 63.94 | 63.94 | 63.94 | 63.94 | 63.94 | 63.94 |
| **Functional monomers (mM)** | AA | - | 100 | - | - | - | 100 | - | - | - |
| | MAA | - | - | 100 | - | 100 | - | 100 | - | 100 |
| | 4-VP | - | - | - | 100 | 100 | - | - | 100 | 100 |
| **Drugs (mM)** | MXF* | - | - | - | - | - | 5.71 | 5.71 | 5.71 | 5.71 |
| | DFN* | - | - | - | - | - | 7.86 | 7.86 | 7.86 | 7.86 |

*The molar concentrations of MXF and DFN are different, to keep the same masses of the drugs.

### 2.2.2. Drug loading and release experiments

The drug loading was done by soaking the disks or the dumbbell-shaped specimens in 1 or 3 mL, respectively, of a solution of PBS containing both drugs (2.56 mM of MXF and 1.76 mM of DFN), for 14 days at 60 ºC. The selection of the loading conditions (14 days at 60ºC) was based on previous studies (Topete et al., 2019, 2018) where they were found to improve loading without the risk of drug degradation. The concentrations of the drugs, were the maximum possible values, since the solubility of DFN in saline solutions, when combined with MXF, is low. Sterilization was carried out on the last day of drug loading by high hydrostatic pressure (HHP) at 600 MPa, 70 ºC for 10 min, using a high pressure equipment (Hiperbaric 55, Burgos, Spain). Before pressurization, the samples were pre-heated at the same temperature for 10 min. Sterilization conditions were also optimized in a previous work (Topete et al., 2020).

*In-vitro* drug release experiments were done in sink conditions by immersing the drug-loaded disks in 3 mL of PBS solution, at 36 ºC and 180 rpm in a shaker (Incubating Mini Shaker, VWR). At pre-determined times, aliquots of 0.3 mL of the supernatant were removed and replaced by the same amount of fresh PBS solution. To calculate the amount of drug released, the concentration of both drugs was calculated from the absorbance of the removed aliquots read using an UV-Vis spectrophotometer (MultiscanGO, ThermoScientific®). Proper dilutions with PBS were made when necessary. The entire spectra (200-700 nm) were acquired and a deconvolution method described by Kim and Chauhan (Kim and Chauhan, 2007), based on the spectra of standard single drug solutions, was used. The experiments were done, at least, in triplicate.

The total amount of drug loaded into the samples was determined through an extraction procedure with ethanol. The drug-loaded samples were placed inside vials with 3 mL of ethanol/sample. After pre-determined times, the ethanol solution was analyzed by UV-Vis spectroscopy and replaced with fresh ethanol solution. This procedure was carried on until no drug was detected in the ethanol solution. The cumulative amount of drug was calculated.

.

### 2.2.3. Prediction of the *in vivo* therapeutic efficacy

To predict the drug concentration in the aqueous humor resultant from the release of the drug-loaded IOLs a mathematical model described by Pimenta *et al.* (Pimenta et al., 2018) was used. The model assumes for simplification that the drug-loaded IOL has a flat 2D geometry, with thickness 2l, being x = 0 the center of the lens. The IOL is implanted in the capsular bag, permeable to the small drug molecules (Danysh and Duncan, 2009; Davis, 1974; Kastner et al., 2013). Half of the drug released by the IOL diffuses freely to the vitreous ($x \leq -l$), while the other half diffuses to the aqueous humor ($x \geq l$), and can penetrate into the cornea or be washed out by the aqueous humor turnover. The drug concentration in the aqueous humor ($C_{aq}$) over time can be estimated through the following equation:

$$V_{aq}\frac{dC_{aq}}{dt} = A_{surf}D_e\left|\frac{\partial C}{\partial x}\right|_{x=l} - (k_{cornea}A_{cornea} + r)C_{aq} \qquad \text{(Eq. 1)}$$

which considers that the accumulation of drug in the aqueous humour is the difference between the drug released from the IOL of surface area $A_{surf}$ and thickness $2l$ = 0.6 mm into the aqueous humor ($A_{surf}D_e\left|\frac{\partial C}{\partial x}\right|_{x=l}$, where $D_e$is the effective diffusivity) and the drug that lost due to penetration in the cornea ($k_{cornea}A_{cornea}C_{aq}$) and due to the aqueous humor renovation ($rC_{aq}$). The values of the cornea permeability ($k_{cornea}$) for the studied drugs were taken from literature: $1.58 \times 10^{-6}$ cm.s$^{-1}$ for MXF (Robertson et al., 2005) and $2.65 \times 10^{-7}$ cm.s$^{-1}$ for DFN (Valls et al., 2008); the area of the cornea ($A_{cornea}$) was assumed to be 1.3 cm$^2$ (Naumann and Apple, 1986); the aqueous humor turnover ($r$) was 2.5 µL.min$^{-1}$ and its volume $V_{aq}$ = 250 µL (Cholkar et al., 2013). The effective diffusivity ($D_e$) was calculated by fitting the experimental data of the release tests using the procedure described by Pimenta *et al.* (Pimenta et al., 2016), assuming valid the Fick's second law (see Figure S1, Supplementary information). The following equations were set to account for the symmetry at the lens center (Eq. 2), the sink conditions assumption at the vitreous-IOL boundary (Eq. 3) and the equilibrium between the drug concentration in the aqueous humor ($C_{aq}$) and in the lens considering the drug partition coefficient ($K$) (Eq. 4).

$$\frac{\partial C}{\partial x}(x=0,t)=0 \qquad \text{(Eq. 2)}$$

$$C(x=-l,t)=0 \qquad \text{(Eq. 3)}$$

$$C(x=l,t)=KC_{aq} \qquad \text{(Eq. 4).}$$

The initial conditions for the drug concentration in the aqueous humor and inside of the drug-loaded lens are, respectively:

$$C_{aq}(t=0)=0 \qquad \text{(Eq. 5)}$$

$$C(x,t=0)=C_i(x) \qquad \text{(Eq. 6)}$$

The partition coefficient ($K$) was calculated using the following equation:

$$K=\frac{C_{lens}}{C_{sol}} \qquad \text{(Eq. 7)}$$

through the determination of the concentration of drug inside the drug-loaded lens, $C_{lens}$, and the concentration of the loading solution when in equilibrium with the drug-loaded lens, $C_{sol}$. $C_{lens}$ was calculated by dividing the total amount of drug-loaded into the lens by the lens volume.

### 2.2.4. Physico-chemical characterization of the hydrogels

#### 2.2.4.1. Liquid uptake

To evaluate the liquid uptake of the samples, first, the weight of the dry disks was measured. Then, the disks were immersed in 1 mL of the testing solution (PBS or drug solution) until equilibrium was achieved. The disks were removed from the solution, gently blotted with paper to remove the excess of liquid present on their surface and weighted again. The liquid uptake percentage (%LU) was calculated through the following equation:

$$\%LU = \frac{W_t - W_0}{W_0} \times 100 \qquad \text{(Eq.8)}$$

where $W_t$ is the weight of the hydrated disks and $W_0$ is the weight of the dry disks. The experiment was done at least in triplicate.

#### 2.2.4.2. Transmittance

The transmittance of the samples hydrated in PBS or in drug solution was determined in the wavelength interval of 300-650 nm using an UV–vis spectrophotometer (Multiskan GO, ThermoScientific). At least, three different measurements were done in three distinct samples of each type.

#### 2.2.4.3. Elastic Modulus

The elastic modulus was obtained through tensile tests carried out with the dumbbell samples in the TA.XT Express Texture Analyser (Stable Micro Systems). The software Exponent was used to collect the data. The samples were hydrated in PBS or in drug solution. The elastic modulus was calculated from the initial slope of the obtained stress-strain curves. The trigger force used was 0.005 N and the test speed was 0.3 $mm.s^{-1}$. At least, five different experiments were done per type of sample.

#### 2.2.4.4. Molecular structure

To analyze the molecular structure of the materials, the Fourier-Transform Infrared spectroscopy - Attenuated Total Reflection (FTIR-ATR) technique was employed. The samples were first hydrated in PBS or drug-loaded and then dried for 7 days, at 36ºC in a vacuum oven. A Smart iTR™ sampling accessory mounted on a Nicolet 5700 FTIR spectrometer (Thermo Electron Corporation, USA) was used with 128 scans and a resolution of 4 $cm^{-1}$. At least, two different samples per type were analysed.

### 2.2.5. Irritability tests

To assess the potential of the materials for ophthalmic irritability, the Hen's Egg Test on the Chorioallantoic Membrane (HET-CAM) was carried out using fertilized chicken eggs (Sociedade Agrícola da Quinta da Freiria, SA, Portugal). The eggs were incubated (Intelligent Incubator 56S) at 37 ºC and 60 % of relative humidity. On day 9 of incubation, the eggs were removed and placed with the wider extreme upwards. A circular cut at the air chamber zone of the egg was done with a Dremel® 3000 rotary tool (Dremel Europe, Breda, Netherlands). The inner membrane was moistened with NaCl solution (0.154 M) and the eggs were incubated for 30 minutes more. Next, the NaCl solution was removed, and the inner membrane was carefully removed with a tweezer, ensuring that the chorioallantoic membrane remained intact. The disks to be tested were

applied directly on the chorioallantoic membrane. The disks were hydrated in PBS or drug solution and were sterilized by HHP before the test. As negative and positive controls, 300 µL of NaCl (0.154 M) and NaOH (0.1 M), respectively, were used. The membranes were observed for 5 minutes, for the appearance of coagulation, vascular lysis or haemorrhage. At least, a triplicate was done for each type of sample and control.

### 2.2.6. Cytotoxicity tests

The cytotoxicity of the disks was studied by indirect contact with NIH/3T3 fibroblasts (93061524) obtained from Health Protection Agency Culture Collections and supplied by Sigma using porous cell culture inserts (Transwell®), according to the international standard (ISO 10993-5, 2009). The cells were cultured in DMEM supplemented with 1% penicillin-streptomycin solution and 10% calf serum. After growing, the cells were harvested and a calculated quantity of DMEM was added to obtain a density of $1 \times 10^5$ cells/well. A volume of 600 µL of the cells+DMEM mixture was added to each well of a 24-well culture plate. Then, the plate was incubated for 24 h at 37 °C under a humidified atmosphere containing 5 % $CO_2$ in air. The culture inserts and the disks, hydrated in PBS or in drug solution and sterilized by HHP were placed above the wells. To ensure that the materials were completely immersed, extra 100 µL of DMEM was poured on the top of each disk. As negative control was used DMEM, while the positive control was DMEM with 7.5% of DMSO to ensure that cells die in the presence of a toxic drug. The plates were further incubated for 24 h at 37° C under a humidified atmosphere containing 5 % $CO_2$. On the following day, the inserts with the disks and the medium were removed and 300 µL of MTT solution (0.5 mg/mL in serum-free DMEM) were added. The plates were incubated once more for 3 h in the conditions described previously. Next, 450 µL of MTT solvent (IGEPAL at 0.1 %, prepared in isopropanol with 4 mM HCl) were added to each well and the plates were shaken until complete homogenization and dissolution of the formazan crystals that were formed. To determine the cellular viability, the absorbance of each well was measured at 595 nm using a microplate reader (Platos R 496). The cellular viability was determined comparing the values of the measured absorbance with the negative control, which is considered 100% of cellular viability. At least, five disks were tested for each experimental condition. Adhesion and morphology of the cells was observed using an inverted light microscope Axiovert 25 (Zeiss, USA).

### 2.2.7. Antibacterial tests

The antibacterial activity of the released MXF against *S. aureus* (ATCC 25923) and *S. epidermidis* (CECT 231) was assessed through agar diffusion tests. Both bacteria were streaked and incubated at 37 ºC for 24 h. Colonies of each bacteria were inoculated in different sterile solutions of NaCl (0.9 %) until an optical density of 1 McFarland was achieved. MH agar was prepared and sterilized by autoclave, according to the manufacturer instructions, and stabilized at 50 ºC in a water bath before using. Thereafter, 350 µL of bacteria were added to 50 mL of MH agar, gently mixed, and carefully poured into petri dishes (120x120 $mm^2$) avoiding the formation of air bubbles. After solidification, blank susceptibility disks were placed above the agar surface mixture and 15 µL of the testing solution or of PBS (negative control) was pipetted into them, to ensure complete liquid absorption. The plates were incubated at 37 ºC for 24 h. The formed inhibition halos around the disks were measured with an electronic caliper. A calibration curve was obtained for each bacteria with solutions of MXF of known concentration to relate the drug concentration with the diameter of the produced inhibition halos. The concentration determined from the inhibition halos was compared with the concentration calculated from UV-VIS spectroscopy to infer about the eventual activity loss of the released MXF.

#### 2.2.8. Statistical analysis

The software IBM SPSS Statistics was used to perform the statistical analysis. The Shapiro-Wilk test was used to check for normality. When normality was followed, t-test was used to compare two groups of samples, while one-way analysis of variance (ANOVA) was used when more than two groups were considered. In this case, the identification of the groups with different means was done using the Bonferroni Post-Hoc test. When normality was not verified, non-parametric tests were performed using a Mann-Whitney test or a Kruskal-Wallis test. The level of significance used was 0.05.

## 3. Results

### 3.1. Drug release profiles

**Figures 2** and **3** present, respectively, the MXF and DFN release profiles from the dual drug-loaded hydrogels. Each graphic compares the profiles obtained with three different hydrogels: blank hydrogel, hydrogels with functional monomers, and drug imprinted hydrogels.

For MXF (**Figure 2**), it is clear the effect of the functional monomers on the release profiles. The best results were obtained with the monomer MAA, which led to a controlled and extended drug release for at least 14 days, while the monomer 4-VP did not influence the release, at all. In contrast, molecular imprinting practically did not affect the release. The only exception was the case of monomer AA where the release profiles obtained with HA and HA-I are slightly different ($p$-value = 0.000).

For DFN (**Figure 3**) the effect of the presence of the monomers on the release profiles was small, compared to that observed for MXF, being the best results obtained with MAA. Again, molecular imprinting almost did not change the release profiles.

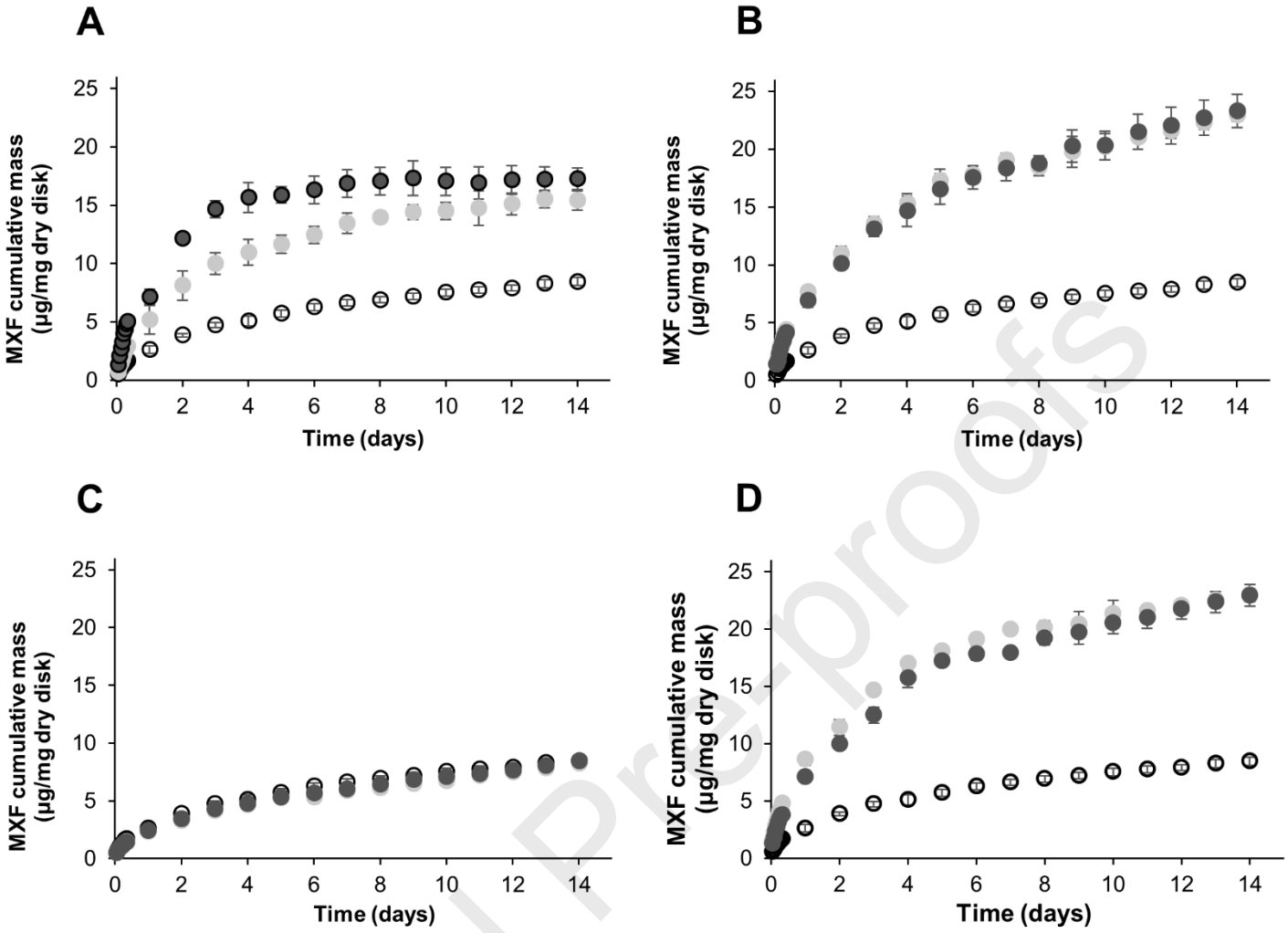


**Figure 2.** Release profiles of MXF obtained with: blank hydrogel (○), hydrogels with functional monomers (●) and drug imprinted hydrogels (●). The effect of the different monomers is compared: **A)** AA, **B)** MAA, **C)** 4-VP and **D)** MAA + 4-VP.

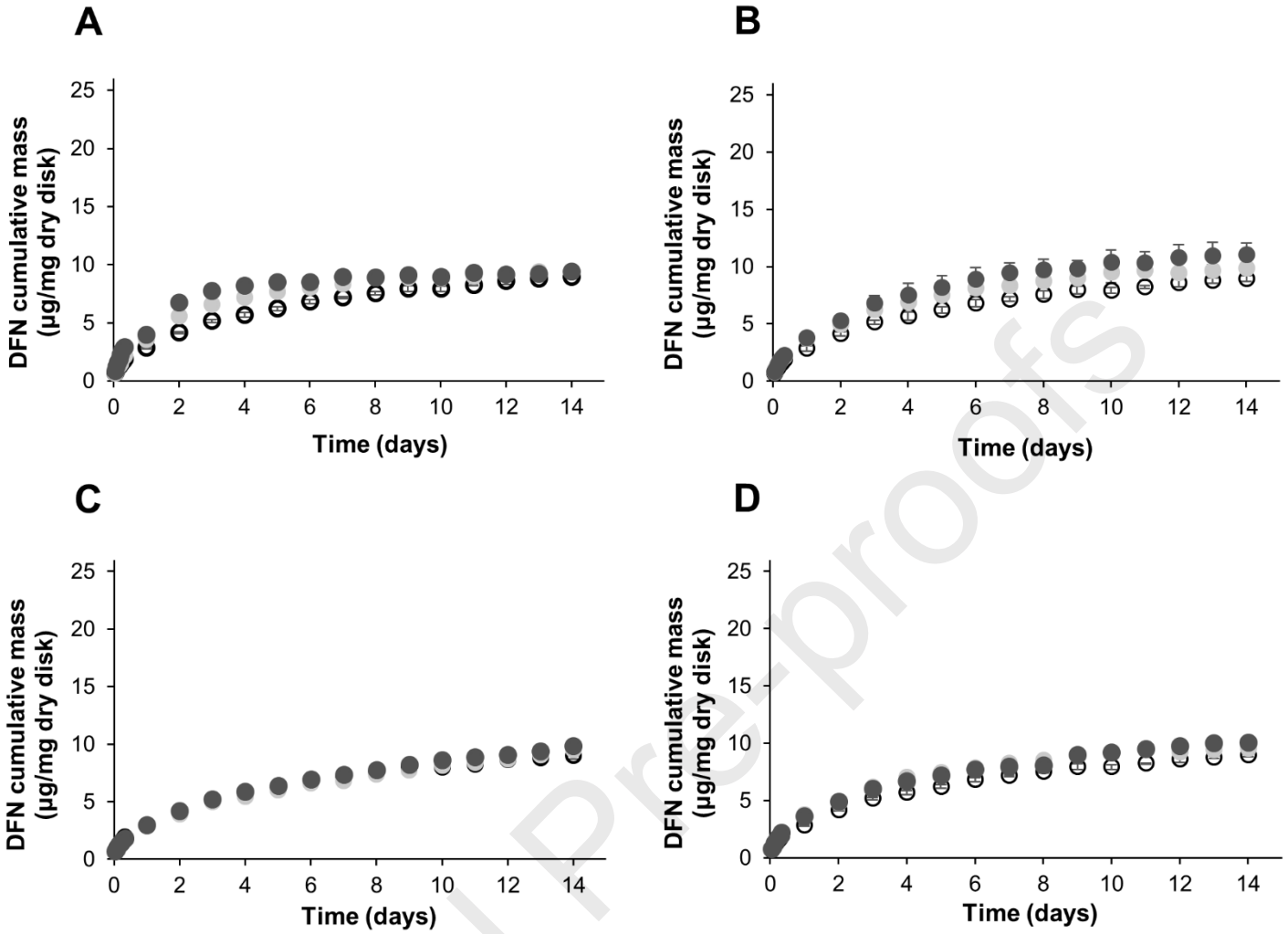


**Figure 3.** Release profiles of DFN obtained with: blank hydrogel (○), hydrogels with functional monomers (●) and drug imprinted hydrogels (●). The effect of the different monomers is compared: **A)** AA, **B)** MAA, **C)** 4-VP and **D)** MAA + 4-VP.

**Table 2** shows the amount of drug-loaded into each hydrogel as well the corresponding percentage released after 14 days. In the case of MXF, the amount of drug-loaded and the % of drug released increased significantly when the hydrogels were functionalized with all the monomers ($p$-value = 0.025 and 0.000 for HA, 0.003 and 0.000 for HM and 0.005 and 0.000 for HMV, respectively), with the exception of 4-VP ($p$-value = 0.315 and 0.060). Molecular imprinting did not affect significantly both the drug loading ($p$-value = 0.940 for HM, 0.920 for HV and 0.821 for HMV), except for HA ($p$-value = 0.012), and the % released ($p$-value = 0.513 for HM, 0.346 for HV and 0.582 for HMV), again except for HA ($p$-value = 0.000). The results obtained with DFN are different. The amount of drug-loaded decreased for the functionalized hydrogels, while the % of drug released increased. The influence of molecular imprinting was not clear because sometimes the errors are large, but, in general, it was not relevant.

The hydrogels HMV and HMV-I released the maximal % of loaded MXF, while HM released the maximal % of loaded DFN. Considering that HM also delivered a high % of MXF, it was considered the best option and we decided to pursue the work with this hydrogel.

**Table 2.** Amounts of drug-loaded and percentages of drug released for the different hydrogels compositions.

| Hydrogel | Amount of drug-loaded (μg/mg dry gel) | | Percentage of drug released after 14 days | |
|---|---|---|---|---|
| | Drugs | | Drugs | |
| | MXF | DFN | MXF | DFN |
| H | 15 ± 2 | 20 ± 3 | 55 ± 2 | 45 ± 1 |
| HA | 20 ± 2 | 14.4 ± 0.7 | 77 ± 1 | 65 ± 1 |
| HA-I | 25 ± 1 | 15 ± 2 | 69 ± 1 | 64 ± 1 |
| HM | 28 ± 3 | 12.2 ± 0.7 | 81 ± 2 | 81 ± 4 |
| HM-I | 28 ± 3 | 16± 3 | 83 ± 5 | 71 ± 7 |
| HV | 14 ± 2 | 19± 3 | 59 ± 3 | 51 ± 1 |
| HV-I | 14 ± 2 | 17.8 ± 0.7 | 61 ± 3 | 55 ± 3 |
| HMV | 25 ± 3 | 17 ± 1 | 90 ± 2 | 57 ± 3 |
| HMV-I | 25 ± 1 | 13.9 ± 0.80 | 92 ± 4 | 72 ± 4 |

The effect of sterilization by HHP on the release profiles of MXF and DFN from the dual drug-loaded HM hydrogel is shown in **Figure 4**. HHP slightly increased the amount of MXF released (**Figure 4A**, 21 %, *p*-value = 0.001), but did not change the amount of DFN released (**Figure 4B**, *p*-value = 0.428). A controlled and extended release profile for both drugs was maintained for, at least, 14 days after sterilization. The percentage of drug released/ drug loaded is also presented in the **Figure 4C** and **4D** for MXF and DFN, respectively. HHP slightly increased the percentage of released amount/ loaded amount for MXF (9%, *p*-value 0.029) while for DFN no differences were detected (*p*-value of 0.391).

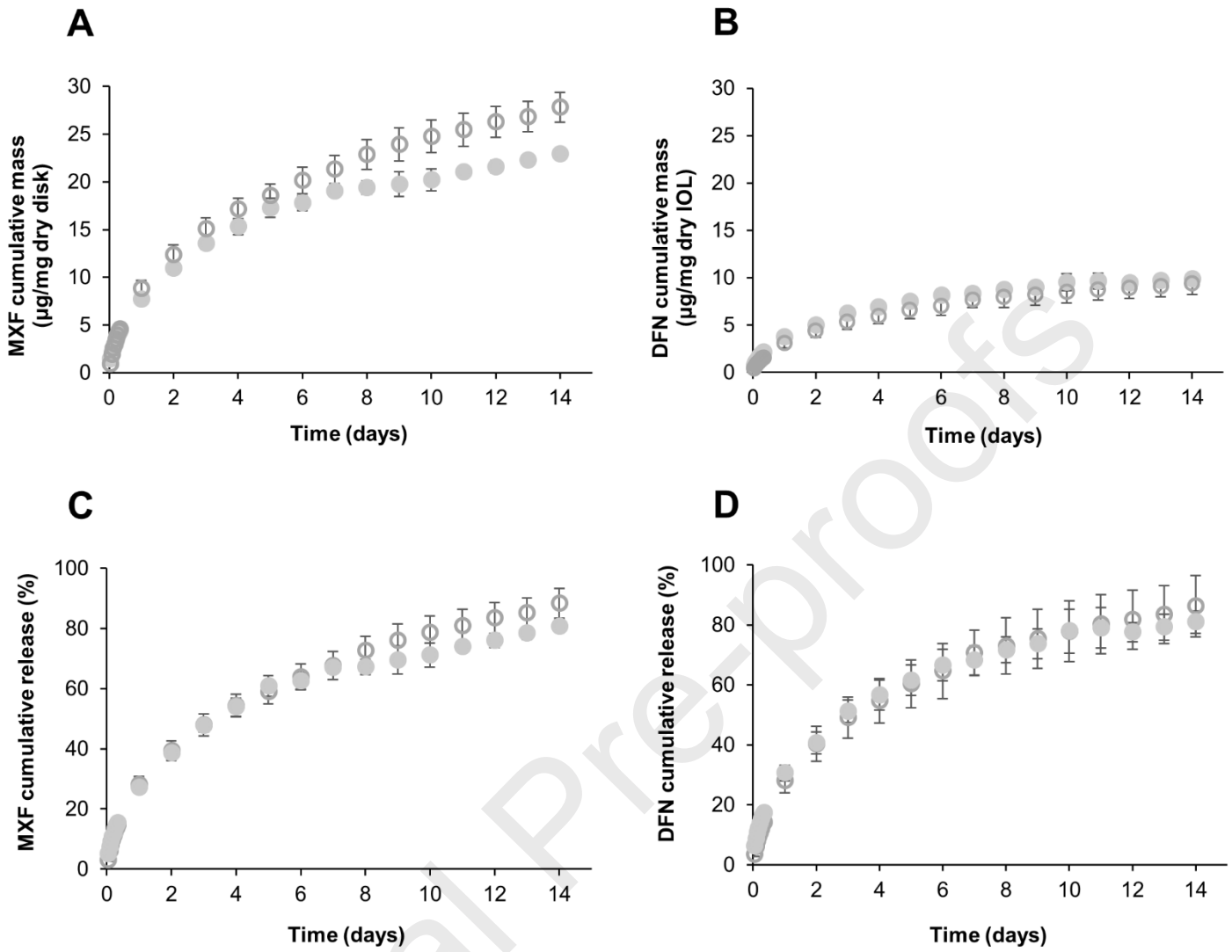


**Figure 4.** Release profiles obtained from HM disks without sterilization (●) and with HHP sterilization (○) for MXF in **A**) µg/mg dry disk and in **C**) % of drug loaded, and for DFN in **B**) µg/mg dry disk and in **D**) % of drug loaded.

### 3.2. Prediction of the *in vivo* therapeutic efficacy

To predict if the system under study would be effective at therapeutic level, a mathematical model, proposed by Pimenta *et al.* (Pimenta et al., 2018), that estimates the drug concentration in the aqueous humor after implantation of a drug-loaded intraocular lens was applied. The estimated concentrations for MXF and DFN along the time are presented in the **Figure 5A** and **5B**, respectively. The concentration of MXF was compared with the minimum inhibitory concentrations (MICs) of *S. aureus* and *S. epidermidis* previously determined in our lab (2 µg/mL) (Topete et al., 2019). The concentration of DFN was compared with the values found in the literature for the half-maximal inhibitory concentration (IC50) of cycloxygenase-1 (COX-1) and cyclooxygenase-2 (COX-2), two enzymes responsible for inflammation (Kim, 2011).

The MXF concentration remained higher than the MICs till the 9$^{th}$ day of release. Concerning DFN, the estimated concentration stayed above both IC50 of COX-1 and COX-2 minimum values for, at least, 14 days.

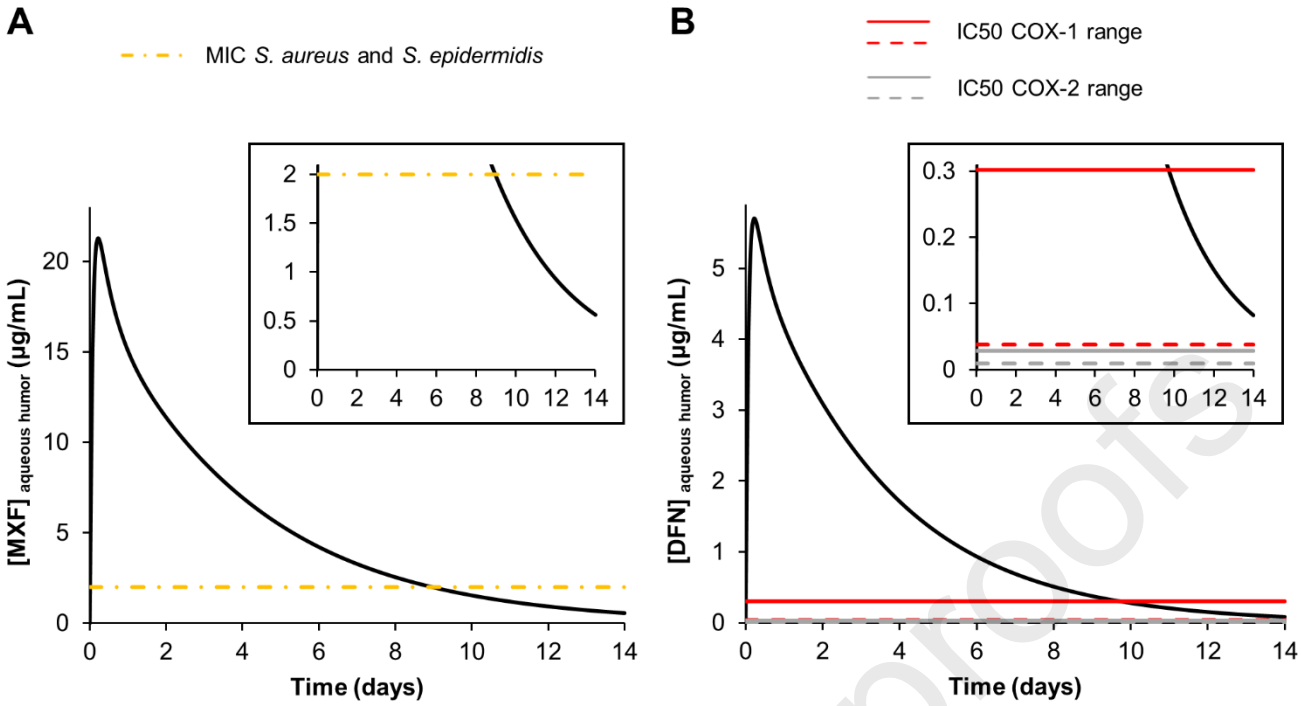


**Figure 5.** Estimated concentration profiles for MXF (**A**) and DFN (**B**) in the aqueous humor,for MXF+DFN loaded-HM loaded lenses after sterilization by HHP. For MXF (**A**) it is presented the MIC of *S. aureus* and *S. epidermidis* (Topete et al., 2019). For DFN (**B**) it is presented the range found in the literature for IC50 COX-1 and COX-2 (Kim, 2011).

### 3.3. Physico-chemical properties

The effect of the MAA addition, loading with MXF+DFN and HHP sterilization on the physico-chemical properties of the CI26Y material, was evaluated.

The liquid uptake capacity and the Young's modulus for the hydrogels H, HM, HM loaded with MXF+DFN, and the latter submitted to HHP sterilization, are presented in **Figures 6A** and **6B**, respectively. The most significant increase in liquid uptake (around 25%) was observed for the drug-loaded HM disks after sterilization ($p$-value = 0.000). H disks equilibrated with PBS presented a Young's modulus ≈ 44 % higher than those of all other tested disks.

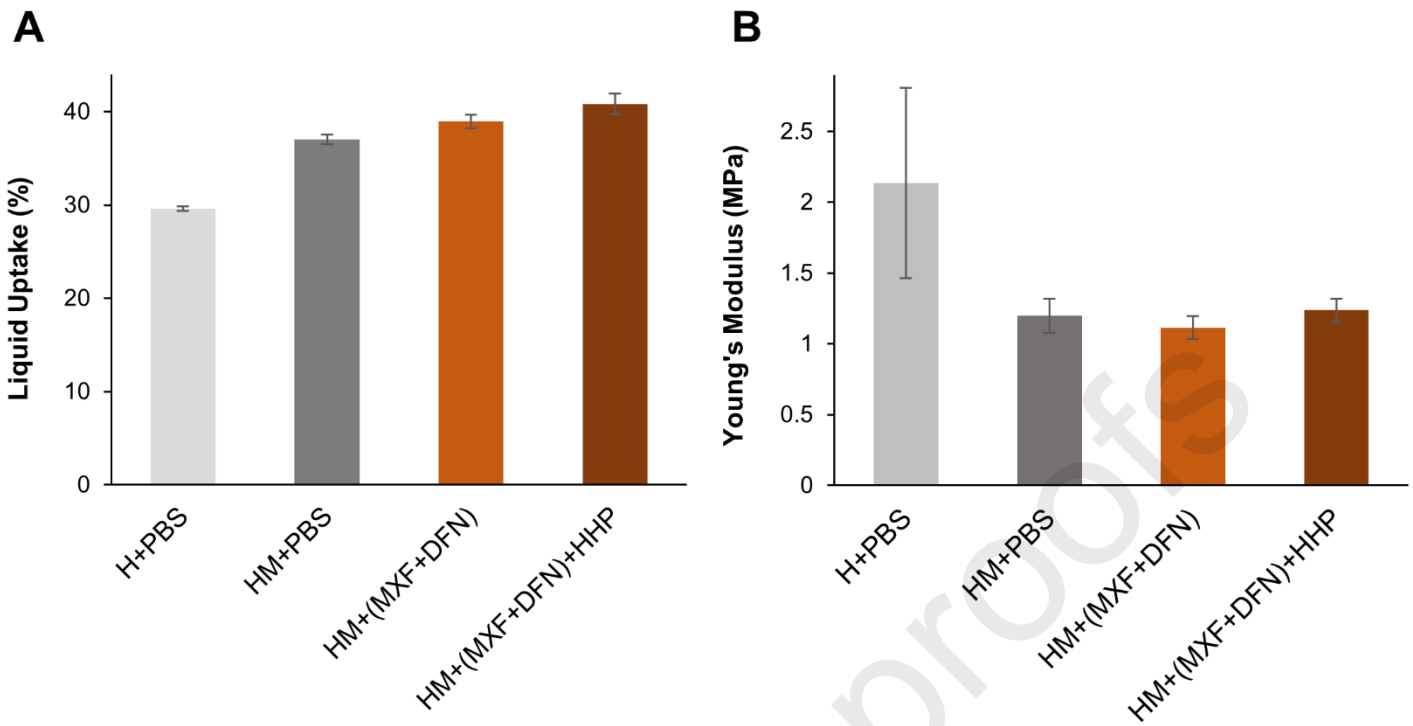


**Figure 6. (A)** Liquid uptake (%) and **(B)** Young's modulus (MPa) obtained for: H disks hydrated in PBS, HM disks hydrated in PBS, HM disks loaded with MXF+DFN, and HM disks loaded with MXF+DFN and sterilized by HHP.

The transmittance of the samples in the wavelength range 300-650 nm is presented **in Figure 7**. Above 500 nm, the transmittance of all disks is higher than 90%. In the region of 350-450 nm, the transmittance of the disks loaded with MXF+DFN decreased in relation to that of the disks hydrated in PBS.

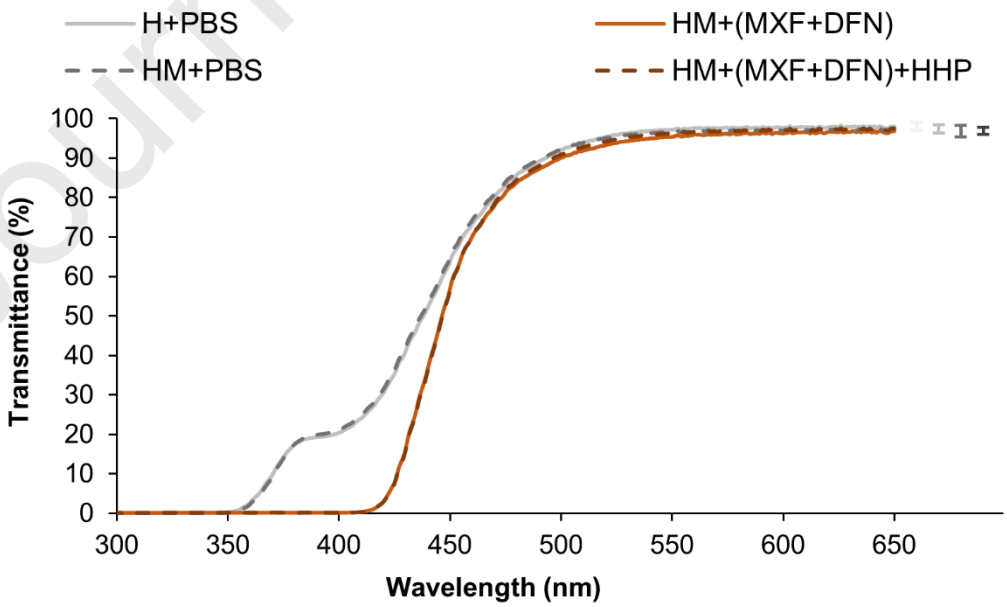

**Figure 7.** Light transmittance (%) of H disks hydrated in PBS, HM disks hydrated in PBS, HM disks loaded with MXF+DFN and HM disks loaded with MXF+DFN and sterilized by HHP.

The FTIR-ATR spectra for the different materials are compared in **Figure 8**. No differences can be found between the spectra of H disks and HM disks hydrated in PBS. However, for HM disks equilibrated with MXF+DFN solution, with or without HHP sterilization, peak appeared around 1620 $cm^{-1}$. These peaks correspond to an alkenyl C=C stretch and its appearance is due to the increase in the number of these bounds when the drugs were loaded into the polymeric matrix. Also a small peak in the region around 800 $cm^{-1}$ becomes evident. Since carbon-chlorine bonds absorb around this value, this peak may be attributed to the presence of MXF hydrochloride into the polymeric matrix.

.

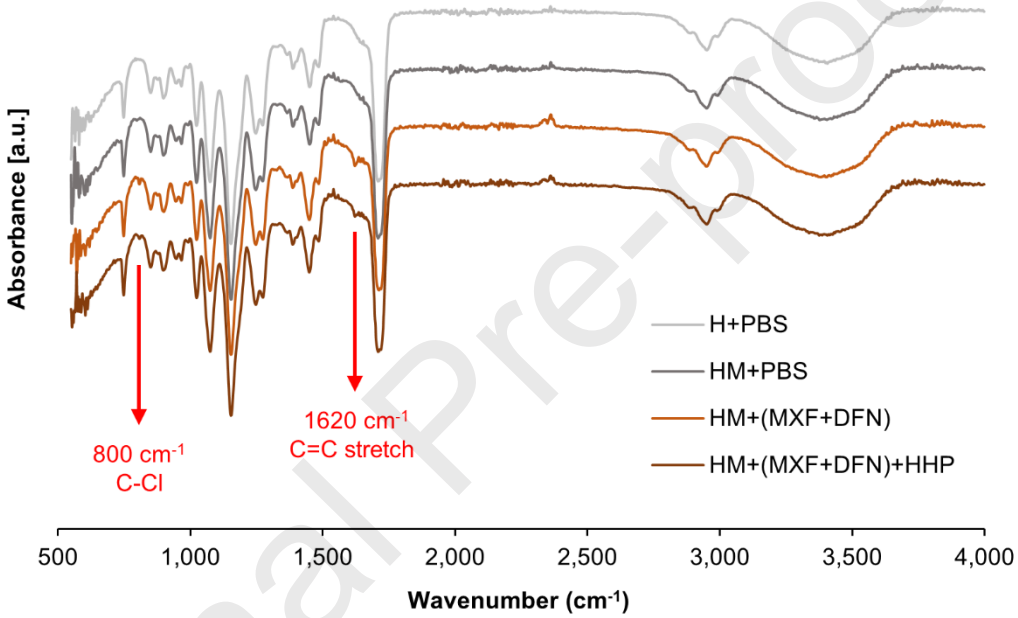


**Figure 8.** FTIR-ATR spectra of H disks hydrated in PBS, HM disks hydrated in PBS, HM disks loaded with MXF+DFN, and HM disks loaded with MXF+DFN and sterilized by HHP.

### 3.4. Irritability tests

The HET-CAM assay was used to predict the irritability of the produced materials on the eye. For this test, all materials were sterilized by HHP, so only three hydrogels were compared: H hydrated in PBS, HM hydrated in PBS and HM loaded with MXF+DFN. The disks were placed in direct contact with the chlorioallantoic (CAM) membrane of fertilized eggs for 5 minutes and the results are depicted in **Figure 9**.

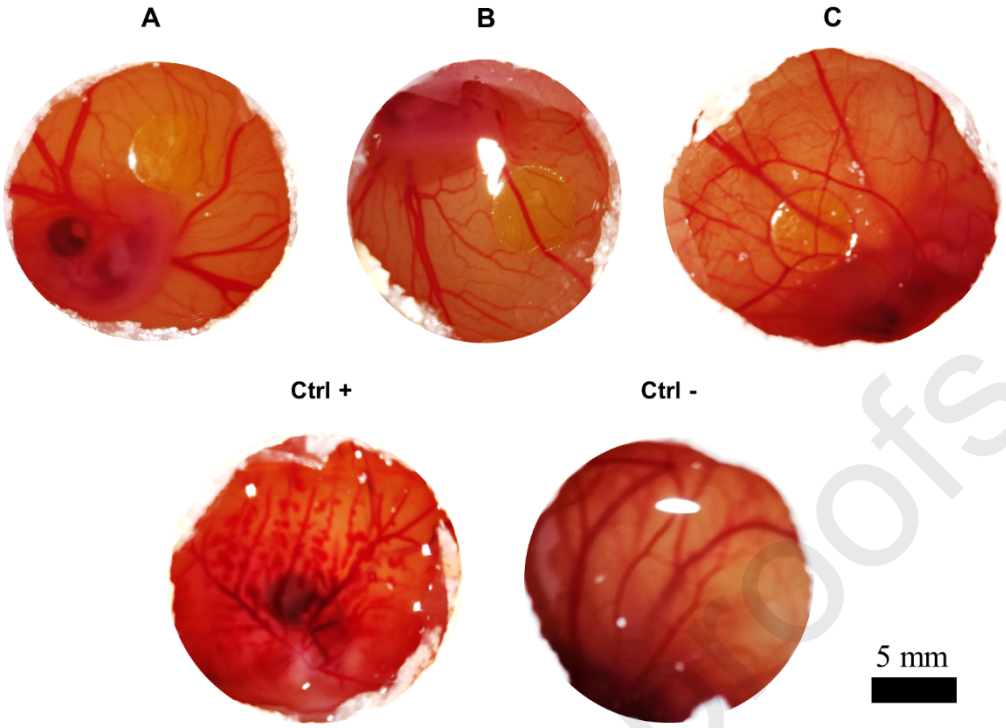


**Figure 9.** Hen's egg chorioallantoic membrane test with H disks hydrated in PBS **(A)** and with HM disks hydrated in PBS **(B)** and loaded with MXF+DFN **(C)**, all sterilized by HHP. The positive (Ctrl +) and negative (Ctrl -) control are also shown.

Careful inspection of the CAM, did not show any sign of lysis, coagulation or haemorrhage in any of the cases, being the membrane similar to that observed in the negative control.

### 3.5. Cytotoxicity tests

The cytotoxicity of the H disks hydrated in PBS, HM disks hydrated in PBS and HM disks loaded with MXF+DFN, all sterilized by HHP, was analysed by indirect contact using NIH/3T3 fibroblasts. The cellular viability was normalized to the negative control, and is displayed in **Figure 10**, as well as images of the cell cultures after incubation with the disks. The cellular viability was 100 ± 5 % for H disks hydrated in PBS, decreasing to 91 ± 6 % for HM disks hydrated in PBS ($p$-value = 0.036) and 84 ± 6 % for HM disks loaded with MXF+DFN ($p$-value = 0.012). The images of the cell cultures for all hydrogels show a high density of adherent fibroblasts with its typical elongated shape morphology with regions of extensively spread cytoplasm, similar to the images observed in the negative control and quite different from the positive control were adhesion and cell density are very low.

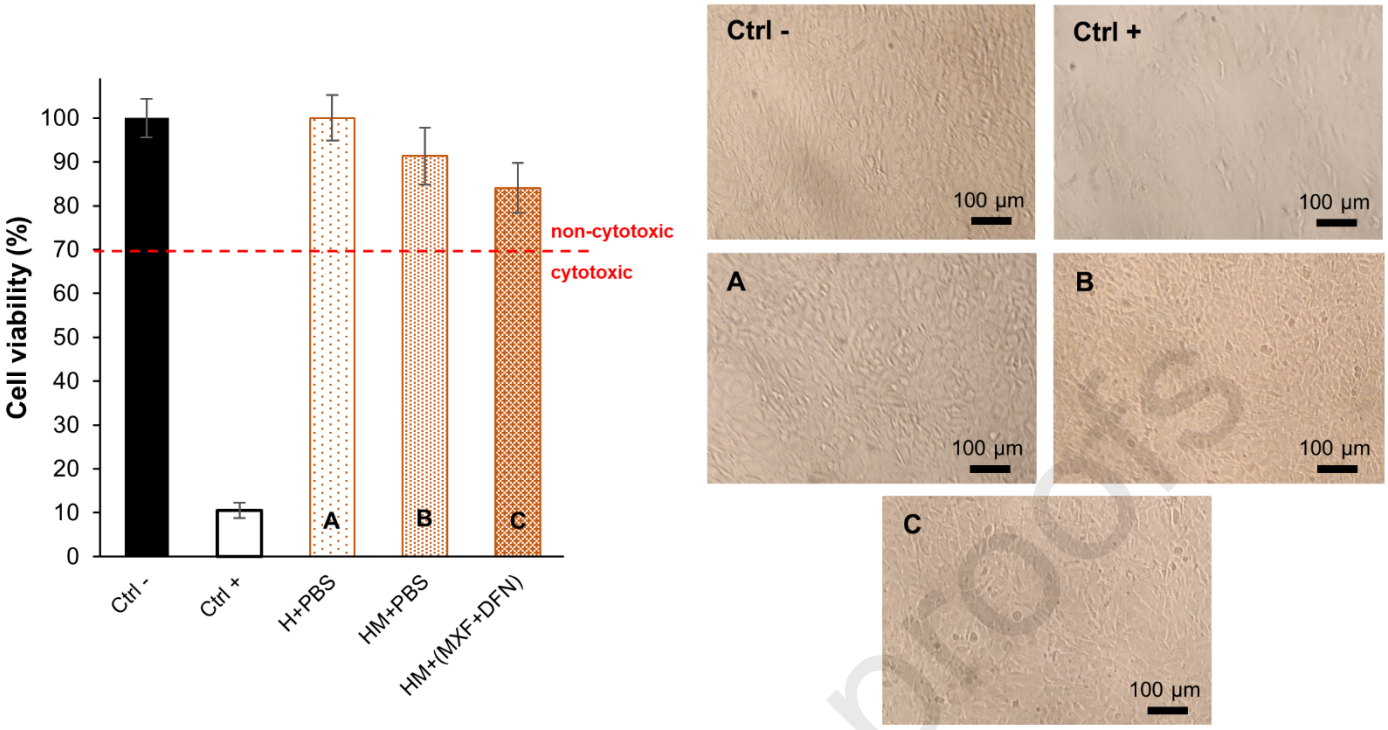


**Figure 10.** Viability and NIH/3T3 cell culture images after incubation for 24 h with H disks hydrated in PBS **(A)** HM disks hydrated in PBS **(B)** and HM disks loaded with MXF+DFN **(C)**, all sterilized by HHP. The results for the negative (Ctrl -) and positive (Ctrl +) control are also presented. Morphology of the cells after incubation observed by inverted light microscope is displayed (100x Amp).

### 3.6. Antimicrobial tests

To infer about the eventual activity loss of MXF released from the drug-loaded HM disks sterilized by HHP, aliquots of the supernatant collected after 14 days of release were tested against *S. aureus* and *S. epidermidis*. The concentration obtained from the produced inhibition halos is compared to the concentration calculated from UV-Vis spectrophotometry in **Figure 11**. No statistical differences were detected between the concentration calculated from UV-VIS measurement and from the formed inhibition halos for *S. aureus* ($p$-value = 0.625) and *S. epidermidis* ($p$-value = 0.865).

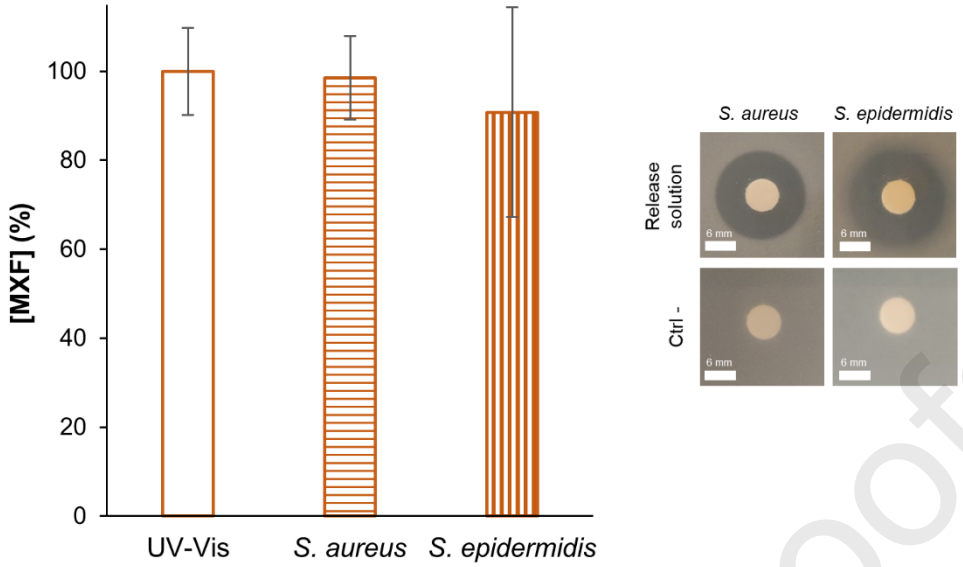


**Figure 11.** MXF concentration of the supernatant solution after 14 days of release from the HM disks loaded with MXF+DFN and sterilized by HHP, determined by UV-vis spectroscopy and from the inhibition halos obtained with *S. aureus* and *S. epidermidis.* Photographs of the inhibition halos obtained with both bacteria are presented, as well as the negative controls (Ctrl-).

## 4. Discussion

In a previous work (Topete et al., 2019), the loading capacity of the acrylic CI26Y material in MXF+DFN by soaking in the dual drug solution demonstrated to be insufficient to ensure a MXF release able to comply with the therapeutic needs. This behaviour resulted, among other factors, from the low concentrations of the drugs in the loading solution (2.56 mM for MXF and 1.76 mM for DFN), which could not be increased due to solubility problems of DFN when dissolved with MXF in the same solution. In the present work, we tried to circumvent this problem, through the addition of different functional monomers to the polymeric matrix, associated or not with a molecular imprinting strategy.

First, the effect of the monomers and of the molecular imprinting was assessed through the comparison of the drug release profiles from the dual drug-loaded hydrogels: H, HA, HM, HV, HMV, HA-I, HM-I, HV-I, and HMV-I (**Figures 2** and **3**). The first conclusion was that no significant differences were detected between the profiles obtained with the functionalized materials and the molecularly imprinted materials, with the exception of HA where a slight increase of 12% was detected for MXF release from HA-I in comparison with HA. A possible reason for the failure of drug imprinting in most of the produced hydrogels may be the concentration of cross-linking agents. In fact, it is reported in the literature (Alvarez-Lorenzo et al., 2010) that sometimes a successful imprinting demands the increase in the amount of cross-linking agent. However, as we used a commercial product, CI26Y, we did not want to change the composition of the starting monomeric mixture. The effect of the monomers was different for both drugs, being much more significant for MXF. Among the various hydrogels, HM showed the greater increase in the amount of MXF loaded (28 µg/mg compared with 15 µg/mg in H), followed by HA. Furthermore, a controlled release of both drugs was obtained with HM for 14 days. The explanation for this behaviour derives from the fact that both AA and MAA monomers have a double bond and a carboxyl group in their chemical composition. MAA has an extra methyl group attached to its alkene group.

Both are widely used in molecular imprinting, since their carboxyl groups can act as hydrogen bond donors or acceptors, and therefore can interact with the target molecule at one or two points. Golker and. Nicholls (Golker et al., 2017) investigated the differences in molecularly imprinted polymers using AA *versus* MAA as functional monomers. They found out that the polymers prepared with MAA presented higher binding capacities than those prepared with AA and attributed it to differences in polymer morphology. AA undergoes auto-accelerated polymerization, as the absence of the methyl group existent in MAA facilitates the attack of the radical center. This leads to differences in the kinetics of the polymerization step and explains the different pore morphologies found in AA-polymers (ink-bottle shaped) and MAA-polymers (slit shaped). Such differences affect the mass transport and the drugs access to the recognition sites, being responsible by the binding qualities of the materials. This can explain the more controlled and extended release of MXF observed in the HM hydrogel. In contrast, the effect of MAA monomer on the loading of DFN was smaller and inverse: the amount of loaded DFN decreased from 20 μg/mg in H to 12 μg/mg in HM**.** One possible reason is the fact that MXF, with eight hydrogen bond acceptors, has a stronger interaction with MAA than DFN, with only three hydrogen bond acceptors. Thus, the preferential interaction of HM with MXF decreases the number of sites available to interact with DFN. Concerning the monomer 4-VP, it did not affect the loading or the release of both MXF and DFN. The fact that the amino group present in 4-VP is not fully protonized in aqueous media (pKa 3.5) (Andrade-Vivero et al., 2007) may be the reason for the weak interactions with the drugs. Besides, hydrophobic bonding between the drug and the pyridine ring of 4-VP through π–π stacking, seems not to play here an important role (Andrade-Vivero et al., 2007). The same effect is visible when combining MAA and 4-VP monomers. The release profiles of MXF and DFN from HM and HMV are quite similar. It is interesting to notice that, despite the similarity of the release profiles, there are differences among the amounts of loaded drug and % drug release from HM and HMV. HM loaded more MXF than HMV and released a smaller percentage. In contrast, HM loaded less DFN than HMV and released a larger percentage. This means that the combination of MAA and 4-VP monomers disfavors the interaction with MXF and favors the interaction with DFN. The results discussed above led us to choose the hydrogel HM as the best option, since a controlled and extended release of MXF and DFN, for at least 14 days, was achieved with the simple addition of MAA to the CI26Y polymeric matrix. As a medical device, the final system needs to be sterile. HHP was the chosen method due to its successful application to drug-loaded IOLs in recent works (Topete et al., 2020). Sterilization slightly increased the final released amount of MXF, while keeping the controlled and extended release, and did not affect the release of DFN.

To predict if the new hydrogel HM, loaded with MXF+DFN and sterilized by HHP, could deliver both drugs at therapeutic levels, a mathematical model was fitted to the obtained drug release profiles. The predicted concentration of MXF in the aqueous humor was above the experimental MICs of *S. aureus* and *S. epidermidis* for 9 days, while that of DFN was above the minimums of IC50 of COX-1 and COX-2, found in literature, for at least 14 days (**Figure 5**). These results meet the requirements of cataract post-operatory prophylaxis, which usually involves the administration of antibiotics for at least 1 week and NSAIDs during 2 weeks (Burling-Phillips, 2013; Haripriya, 2017).

The following step was to investigate the effects of the modifications made in the polymeric matrix upon several properties relevant for the performance of the hydrogels. To address this issue, four intermediate materials corresponding to the several stages of the preparation of the final material were compared: H, HM, HM loaded with MXF+ DFN, and HM loaded with MXF+ DFN and sterilized by HHP. A significant increase in the liquid uptake in PBS and a decrease in the Young's modulus were observed comparing HM with H. This effect has been observed in other polymers (Chhabra et al., 2009), and results from the hydrophilic character of MAA. When HM was loaded with MXF+DFN, the liquid uptake and the Young's modulus did not change significantly. Also, HHP sterilization did not affect the liquid uptake capacity nor the Young's modulus. It must be stressed

that the obtained value for the Young's modulus of the HM hydrogel ensures the flexibility needed for the IOL to be folded when inserted with the injector through a very small incision that is made in the cornea. The light transmittance was reduced in the region of 350-450 nm for the drug-loaded hydrogel, independently of sterilization, due to the presence of MXF. The same reduction was already observed in previous works (Topete et al., 2019, 2018), and, in fact, it can be advantageous to protect the eye against UV-radiation and the blue light of high energy. Above 500 nm the transmittance was always > 90%, which is the value usually reported as the minimum threshold for IOLs (Artigas et al., 2011). FTIR analysis of drug-loaded HM hydrogels revealed the presence of functional groups typical of the drugs, but the spectra of H and HM were very similar, probably due to superposition of the peaks characteristic of the monomer MAA and of the matrix.

The cytotoxicity tests of the hydrogels H, HM and drug-loaded HM, after sterilization, revealed that the tested materials did not induce cellular toxicity. In fact, since the cellular viability is always ≥ 70%, according to the ISO standard (ISO 10993-S, 2009) all materials are considered non-cytotoxic. The high cell spreading and adhesion confirms the cell viability. None of the hydrogels demonstrated irritancy potential by the HET-CAM test, indicating that they are not harmful to the conjunctiva and the cornea.

Finally, antimicrobial tests of the solution released from the dual drug-loaded HM hydrogel, sterilized by HHP, were conducted against *S. aureus* and *S. epidermidis,* and revealed no loss of antibiotic activity.

## 5. Conclusions

In this work, it was demonstrated that it is possible to optimize the simultaneous release of MXF and DFN from the commercial IOL material CI26Y through the addition of an adequate functional monomer. Three monomers were tested: AA, MAA and 4-VP. Besides monomer addition, molecular imprinting with MXF and DFN was also attempted. The hydrogel HM with the monomer MAA and without drug imprinting proved to be the best system, achieving a controlled and extended release for both drugs. A mathematical model applied to the obtained drug release profiles from the sterilized HM hydrogels suggests that the MXF concentration in the aqueous humor shall be above the MIC values of *S. aureus* and *S. epidermidis* for 9 days and the DFN concentration, above the IC50 for COX-1 and COX-2 for 14 days. Microbiological tests demonstrated that the released antibiotic remained active against both bacteria Relevant physical properties of the hydrogels were not significantly affected by the MAA addition, the MXF+DFN loading and the HHP sterilization. In particular, the liquid uptake, the Young's modulus and the optical transmittance were kept within the usual ranges for application in IOLs. Irritability and cytotoxicity tests proved the safety of the produced HM hydrogels.

Finally, the work performed confirms the need for optimizing specifically each lens/drug combination to achieve relevant therapeutic profiles, since the conditions found in a previous work to obtain extended and controlled release of a similar drug pair from the same material (CI26Y), did not work in this case.

**Funding:** This work was supported by Fundação para a Ciência e Tecnologia (FCT) [projects UID/QUI/00100/2019, UIDB/00100/2020, UID/QUI/00062/2019, UIDB/50006/2020 and UIDB/04585/2020 and PhD grant SFRH/BD/139712/2018 and SFRH/BD/137036/2018 from Ana Topete and Carlos A. Pinto, respectively], and, where applicable, co-financed by the FEDER, within the PT2020 Partnership Agreement. Acknowledgements are also due to the project MSC-ETN ORBITAL N° 813440.

**Conflicts of Interest:** The authors declare no conflict of interest.

**References**


Altman, R., Bosch, B., Brune, K., Patrignani, P., Young, C., 2015. Advances in NSAID development: Evolution of diclofenac products using pharmaceutical technology. Drugs 75, 859–877. doi:10.1007/s40265-015-0392-z

Alvarez-Lorenzo, C., Yañez, F., Concheiro, A., 2010. Ocular drug delivery from molecularly-imprinted contact lenses. J. Drug Deliv. Sci. Technol. 20, 237–248. doi:10.1016/S1773-2247(10)50041-8

Anderson, E.M., Noble, M.L., Garty, S., Ma, H., Bryers, J.D., Shen, T.T., Ratner, B.D., 2009. Sustained release of antibiotic from poly(2-hydroxyethyl methacrylate) to prevent blinding infections after cataract surgery. Biomaterials 30, 5675–5681. doi:10.1016/j.biomaterials.2009.06.047

Andrade-Vivero, P., Fernandez-Gabriel, E., Alvarez-Lorenzo, C., Concheiro, A., 2007. Improving the Loading and Release of NSAIDs from pHEMA Hydrogels by Copolymerization with Functionalized Monomers. J. Pharm. Sci. 96, 802–813. doi:10.1002/jps.20761

Aptel, F., Colin, C., Kaderli, S., Deloche, C., Bron, A.M., Stewart, M.W., Chiquet, C., 2017. Management of postoperative inflammation after cataract and complex ocular surgeries: a systematic review and Delphi survey. Br. J. Ophthalmol. 101, 1451–1460. doi:10.1136/bjophthalmol-2017-310324

Artigas, J.M., Felipe, A., Navea, A., Artigas, C., Garca-Domene, M.C., 2011. Spectral transmittance of intraocular lenses under natural and artificial illumination: Criteria analysis for choosing a suitable filter. Ophthalmology 118, 3–8. doi:10.1016/j.ophtha.2010.06.023

Burling-Phillips, L., 2013. Topical NSAIDs: Best Practices for Safe Use [WWW Document]. URL https://www.aao.org/eyenet/article/topical-nsaids-best-practices-safe-use (accessed 9.7.20).

Chhabra, P., Gupta, R., Suri, G., Tyagi, M., Seshadri, G., Sabharwal, S., Niyogi, U.K., Khandal, R.K., 2009. Studies on Development of Polymeric Materials Using Gamma Irradiation for Contact and Intraocular Lenses. Int. J. Polym. Sci. 2009, 1–9. doi:10.1155/2009/906904

Cholkar, K., Dasari, S.R., Pal, D., Mitra, A.K., 2013. Eye: anatomy, physiology and barriers to drug delivery, in: Ocular Transporters and Receptors. Elsevier, pp. 1–36. doi:10.1533/9781908818317.1

D. Silva, H.C. Sousa, M.H. Gil, L.F. Santos, M. Salema Oom, C. Alvarez-Lorenzo, B. Saramago, A.P.S., n.d. Moxifloxacin-imprinted silicone-based hydrogels as soft contact lenses materials for extended release. Submitted.

Danysh, B.P., Duncan, M.K., 2009. The lens capsule. Exp. Eye Res. 88, 151–164. doi:10.1016/j.exer.2008.08.002

Davis, B.K., 1974. Diffusion in Polymer Gel Implants. Proc. Natl. Acad. Sci. 71, 3120–3123. doi:10.1073/pnas.71.8.3120

Eperon, S., Bossy-Nobs, L., Petropoulos, I.K., Gurny, R., Guex-Crosier, Y., 2008. A biodegradable drug delivery system for the treatment of postoperative inflammation. Int. J. Pharm. 352, 240–247. doi:10.1016/j.ijpharm.2007.10.054

Fintelmann, R.E., Naseri, A., 2010. Prophylaxis of Postoperative Endophthalmitis Following Cataract Surgery. Drugs 70, 1395–1409. doi:10.2165/11537950-000000000-00000

Foster, A., Frcophth, F., Farmer, J., Stevens, S., 2000. Vision 2020 : the Right To Sight Vision 2020 : the Cataract Challenge. Community Eye Heal. 13, 17–19.

Garty, S., Shirakawa, R., Warsen, A., Anderson, E.M., Noble, M.L., Bryers, J.D., Ratner, B.D., Shen, T.T., 2011. Sustained Antibiotic Release from an Intraocular Lens–Hydrogel Assembly for Cataract Surgery. Investig. Opthalmology Vis. Sci. 52, 6109. doi:10.1167/iovs.10-6071

Gaudana, R., Ananthula, H.K., Parenky, A., Mitra, A.K., 2010. Ocular Drug Delivery. AAPS J. 12, 348–360. doi:10.1208/s12248-010-9183-3

Golker, K., Olsson, G.D., Nicholls, I.A., 2017. The influence of a methyl substituent on molecularly imprinted polymer morphology and recognition – Acrylic acid versus methacrylic acid. Eur. Polym. J. 92, 137–149. doi:10.1016/j.eurpolymj.2017.04.043

González-Chomón, C., Braga, M.E.M., de Sousa, H.C., Concheiro, A., Alvarez-Lorenzo, C., 2012. Antifouling foldable acrylic IOLs loaded with norfloxacin by aqueous soaking and by supercritical carbon dioxide

technology. Eur. J. Pharm. Biopharm. 82, 383–391. doi:10.1016/j.ejpb.2012.07.007
Gote, V., Sikder, S., Sicotte, J., Pal, D., 2019. Ocular Drug Delivery: Present Innovations and Future Challenges. J. Pharmacol. Exp. Ther. 370, 602–624. doi:10.1124/jpet.119.256933
Hammam, M.A., Wagdy, H.A., El Nashar, R.M., 2018. Moxifloxacin hydrochloride electrochemical detection based on newly designed molecularly imprinted polymer. Sensors Actuators B Chem. 275, 127–136. doi:10.1016/j.snb.2018.08.041
Haripriya, A., 2017. Antibiotic prophylaxis in cataract surgery – An evidence-based approach. Indian J. Ophthalmol. 65, 1390. doi:10.4103/ijo.IJO_961_17
Haripriya, A., Baam, Z.R., Chang, D.F., 2017. Endophthalmitis Prophylaxis for Cataract Surgery. Asia-Pacific J. Ophthalmol. 6, 324–329. doi:10.22608/APO.2017200
Hoffman, R.S., Braga-Mele, R., Donaldson, K., Emerick, G., Henderson, B., Kahook, M., Mamalis, N., Miller, K.M., Realini, T., Shorstein, N.H., Stiverson, R.K., Wirostko, B., 2016. Cataract surgery and nonsteroidal antiinflammatory drugs. J. Cataract Refract. Surg. 42, 1368–1379. doi:10.1016/j.jcrs.2016.06.006
Huang, X., Wang, Y., Cai, J.-P., Ma, X.-Y., Li, Y., Cheng, J.-W., Wei, R.-L., 2013. Sustained Release of 5-Fluorouracil from Chitosan Nanoparticles Surface Modified Intra Ocular Lens to Prevent Posterior Capsule Opacification: An In Vitro and In Vivo Study. J. Ocul. Pharmacol. Ther. 29, 208–215. doi:10.1089/jop.2012.0184
Kastner, C., Löbler, M., Sternberg, K., Reske, T., Stachs, O., Guthoff, R., Schmitz, K.-P., 2013. Permeability of the Anterior Lens Capsule for Large Molecules and Small Drugs. Curr. Eye Res. 38, 1057–1063. doi:10.3109/02713683.2013.803288
Kim, J., Chauhan, A., 2007. Dexamethasone transport and ocular delivery from poly(hydroxyethyl methacrylate) gels. Int. J. Pharm. doi:10.1016/j.ijpharm.2007.11.049
Kim, S., 2011. Critical appraisal of ophthalmic ketorolac in treatment of pain and inflammation following cataract surgery. Clin. Ophthalmol. 5, 751. doi:10.2147/OPTH.S7633
Kleinmann, G., Apple, D.J., Chew, J., Hunter, B., Stevens, S., Larson, S., Mamalis, N., Olson, R.J., 2006. Hydrophilic acrylic intraocular lens as a drug-delivery system for fourth-generation fluoroquinolones. J. Cataract Refract. Surg. 32, 1717–1721. doi:10.1016/j.jcrs.2006.04.033
Lipnitzki, I., Bronshtein, R., Ben Eliahu, S., Marcovich, A.L., Kleinmann, G., 2013. Hydrophilic Acrylic Intraocular Lens as a Drug Delivery System: Influence of the Presoaking Time and Comparison to Intracameral Injection. J. Ocul. Pharmacol. Ther. 29, 414–418. doi:10.1089/jop.2012.0062
Manju, S., Kunnatheeri, S., 2010. Layer-by-Layer modification of Poly (methyl methacrylate) intra ocular lens: Drug delivery applications. Pharm. Dev. Technol. 15, 379–385. doi:10.3109/10837450903262025
Matossian, C., 2020. Noncompliance with Prescribed Eyedrop Regimens Among Patients Undergoing Cataract Surgery—Prevalence, Consequences, and Solutions. US Ophthalmic Rev. 13, 18. doi:10.17925/USOR.2020.13.1.18
Miller, D., 2008. Review of moxifloxacin hydrochloride ophthalmic solution in the treatment of bacterial eye infections. Clin. Ophthalmol. 2, 77. doi:10.2147/OPTH.S1666
Mohajeri, S.A., Malaekeh-Nikouei, B., Sadegh, H., 2012. Development of a pH-responsive imprinted polymer for diclofenac and study of its binding properties in organic and aqueous media. Drug Dev. Ind. Pharm. 38, 616–622. doi:10.3109/03639045.2011.621126
Naumann, G.O.H., Apple, D.J., 1986. Pathology of the Eye. Springer New York, New York, NY. doi:10.1007/978-1-4613-8525-7
Nichols, P., Mortensen, N., Tingy, D., Vasquez, A., Bates, J., 2018. Pharmacokinetics of Molecular Imprinted Hydrogels as Drug Delivery Vehicles. Biochem. Pharmacol. Open Access 07, 1–4. doi:10.4172/2167-0501.1000238
Patel, A., 2013. Ocular drug delivery systems: An overview. World J. Pharmacol. 2, 47. doi:10.5497/wjp.v2.i2.47
Pimenta, A.F.R., Ascenso, J., Fernandes, J.C.S., Colaço, R., Serro, A.P., Saramago, B., 2016. Controlled drug release from hydrogels for contact lenses: Drug partitioning and diffusion. Int. J. Pharm. 515, 467–475. doi:10.1016/j.ijpharm.2016.10.047

Pimenta, A.F.R., Serro, A.P., Colaço, R., Chauhan, A., 2018. Drug delivery to the eye anterior chamber by intraocular lenses: An in vivo concentration estimation model. Eur. J. Pharm. Biopharm. 133, 63–69. doi:10.1016/j.ejpb.2018.10.004

Robertson, S.M., Curtis, M.A., Schlech, B.A., Rusinko, A., Owen, G.R., Dembinska, O., Liao, J., Dahlin, D.C., 2005. Ocular Pharmacokinetics of Moxifloxacin After Topical Treatment of Animals and Humans. Surv. Ophthalmol. 50, S32–S45. doi:10.1016/j.survophthal.2005.07.001

Tan, D.W.N., Lim, S.G., Wong, T.T., Venkatraman, S.S., 2016. Sustained Antibiotic-Eluting Intra-Ocular Lenses: A New Approach. PLoS One 11, e0163857. doi:10.1371/journal.pone.0163857

Tashakori-Sabzevar, F., Mohajeri, S.A., 2015. Development of ocular drug delivery systems using molecularly imprinted soft contact lenses. Drug Dev. Ind. Pharm. 41, 703–713. doi:10.3109/03639045.2014.948451

Topete, A., Oliveira, A.S., Fernandes, A., Nunes, T.G., Serro, A.P., Saramago, B., 2018. Improving sustained drug delivery from ophthalmic lens materials through the control of temperature and time of loading. Eur. J. Pharm. Sci. 117, 107–117. doi:10.1016/j.ejps.2018.02.017

Topete, A., Pinto, C.A., Barroso, H., Saraiva, J.A., Barahona, I., Saramago, B., Serro, A.P., 2020. High Hydrostatic Pressure as Sterilization Method for Drug-Loaded Intraocular Lenses. ACS Biomater. Sci. Eng. 6, 4051–4061. doi:10.1021/acsbiomaterials.0c00412

Topete, A., Serro, A.P., Saramago, B., 2019. Dual drug delivery from intraocular lens material for prophylaxis of endophthalmitis in cataract surgery. Int. J. Pharm. 558, 43–52. doi:10.1016/j.ijpharm.2018.12.028

Valls, R., Vega, E., Garcia, M.., Egea, M.., Valls, J.., 2008. Transcorneal Permeation in a Corneal Device of Non-Steroidal Anti-Inflammatory Drugs in Drug Delivery Systems. TOMCJ 2, 66–71. doi:10.2174/1874104500802010066

White, C.J., Byrne, M.E., 2010. Molecularly imprinted therapeutic contact lenses. Expert Opin. Drug Deliv. 7, 765–780. doi:10.1517/17425241003770098

Zaidi, S.A., 2016a. Molecular imprinted polymers as drug delivery vehicles. Drug Deliv. 23, 2262–2271. doi:10.3109/10717544.2014.970297

Zaidi, S.A., 2016b. Latest trends in molecular imprinted polymer based drug delivery systems. RSC Adv. 6, 88807–88819. doi:10.1039/C6RA18911C

**Authors contributions**

Conceptualization: A. Topete, B.Saramago, A.P. Serro

Methodology: A. Topete, B.Saramago, A.P. Serro

Software: N.A.

Validation: N.A.

Formal Analysis: A. Topete, B.Saramago, A.P. Serro

Investigation: A. Topete, I. Barahona, L.F. Santos

Resources: C.A. Pinto, J.A. Saraiva

Data Curation: A. Topete

Writing – Original Draft Preparation: A. Topete

Writing – Review & Editing: A. Topete, B.Saramago, A.P. Serro

Visualization: A. Topete,

Supervision: B.Saramago, A.P. Serro

Project Administration: A.P. Serro

Funding Acquisition: A.P. Serro

**Declaration of interests**

☒ The authors declare that they have no known competing financial interests or personal relationships that could have appeared to influence the work reported in this paper.

☐The authors declare the following financial interests/personal relationships which may be considered as potential competing interests:

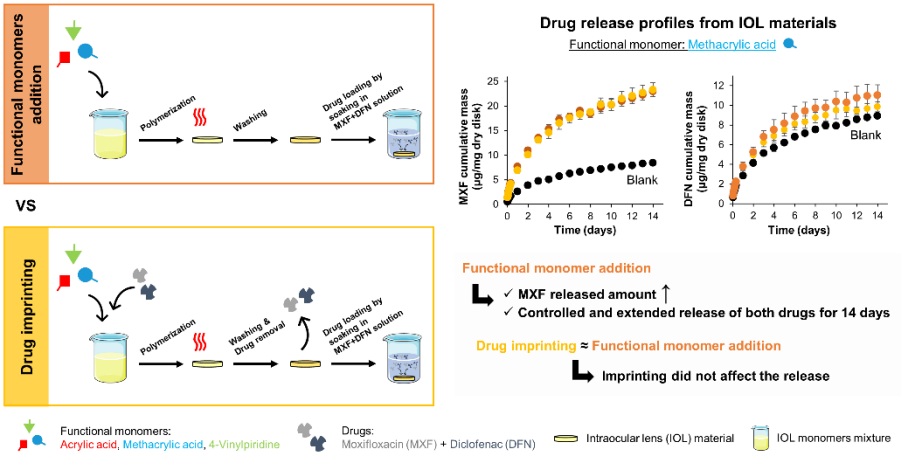

**Highlights**

- Drug release from intraocular lenses (IOLs) materials was optimized by monomer addition
- Addition of methacrylic acid (MAA) to the IOL monomer mixture was the best solution.
- Molecular imprinting of drugs did not led to improvements compared to functional monomer addition
- Drug-loaded MAA-IOLs delivered moxifloxacin and diclofenac at therapeutic levels
- Drug-loaded MAA-IOLs revealed to be non-cytotoxic and non-irritant